

Bandgap Shifting and Crystalline Quality of RF-Sputtered Intrinsic-ZnO Nanofilm for TFSC Application

J. Husna^{1,4}, P. S. Menon^{1*}, P. Chelvanathan², J. Sampe¹, N. Amin³, S. K. Tripathy⁵, T. R. Lenka⁵,
A. R. Md. Zain¹ and M. A. Mohamed¹

¹Institute of Microengineering and Nanoelectronics (IMEN), Universiti Kebangsaan Malaysia.

²Solar Energy Research Institute (SERI), UKM Bangi, Malaysia.

³Universiti Tenaga Nasional (UNITEN), Jalan IKRAM-UNITEN, Selangor, Malaysia.

⁴Department of Electrical Engineering, Islamic University of North Sumatra, Sumatera Utara, Indonesia.

⁵Dept. of Electronics & Communication Engineering, National Institute of Technology Silchar, India.

ABSTRACT

Intrinsic Zinc Oxide (i-ZnO) is a promising material and has been applied in many types of solar cell structures, and particularly in thin film solar cells (TFSC) where it is normally used as the n-type layer or as normally addressed, the buffer or window layer. In this work, ZnO nanofilm was deposited by radio frequency (RF) sputtering technique and the thickness was varied in the range of 50 to 200 nm. The overall results show that the average transmission of i-ZnO was over 70% and the band gap (E_g) obtained was in the range of 3.14 eV-3.25 eV for all nanofilms. Meanwhile, for the structural results, it was clearly shown that the crystalline size of the nanofilms have good quality, and all ZnO films exhibited a (002) diffraction peak, proving the crystallinity of the films via x-ray diffraction (XRD) data analysis. The results assume that the ZnO with various thicknesses deposited with this technique were in accordance with its expected properties and is acceptable to be utilized in TFSC application as a buffer or window layer.

Keywords: Band Gap, Intrinsic Zinc Oxide (i-ZnO), Buffer Layer, Thin Film Solar Cell (TFSC), RF Sputtering.

1. INTRODUCTION

Zinc oxide (ZnO) has been demonstrated as the most promising material for nanoelectronic device application. Over the last decade, ZnO has received high attention due to its unique electrical properties, such as a wide band gap energy (3.37 eV), high excitation binding energy, and large piezoelectric coefficient at room temperature [1-2]. It is well known that ZnO is a promising material and is an important semiconductor which is widely used in the field of solar cell application due to its suitability as both intrinsic n-type buffer layer (i-ZnO) and Al-doped top contact or window layer in solar cell devices [3-6]. Recently, ZnO and ZnO plasmonic nanoparticles have also the potential to be used in anti-influenza drugs such as H1N1 and even possibly in the recent COVID-19 pandemic [7]. In solar cell structures, the window layer usually consist of three thin layers, which are transparent layers with different electrical and optical properties, such as the front contact layer and the buffer layer [8]. All-oxide solar cells are promising candidates for future sustainable energy production and one of the well-known candidate for this application is ZnO. Oxide semiconductors like zinc oxide normally have a wide span of electronic properties, with many of them being abundant, low cost, chemically stable and non-toxic. The excitonic optical absorption mechanism is possible at room temperature for ZnO because the values of ZnO binding energy of 60 meV, but it is still in estimate and need to be

*Corresponding Author: susi@ukm.edu.my

proved by practical observation [9]. ZnO is widely implemented in the field of photovoltaics, optoelectronics (e.g., thin-film displays and light-emitting diodes) and functional coatings (e.g., solar control windows) [8].

Over the years, active research have been executed to discover new effective materials that can possibly be applied as the main layer, contact layer and buffer/window layer, particularly in thin film solar cell (TFSC) structures. In accordance to that, active research work is undertaken to find new methods to deposit these layers. Therefore, the main goal of this work is to find the best technique to deposit these nanofilms which can in turn, effectively decrease the current losses in TFSCs. There are some methods available for the deposition of ZnO including direct current (DC) and radio frequency (RF) sputtering [10], thermal evaporation [11] and reactive ion beam sputtering [12]. In fact, the intrinsic zinc oxide (i-ZnO) in combination with other buffer layers can minimize the interface recombination losses and help to attain a large band-bending [13]. In this work, the thickness of i-ZnO nanofilm layer was varied from 50 to 200 nm in order to investigate the effect of different thicknesses of the buffer layer film. Generally, the material used here was often made from some metal oxides since they can be made transparent and most importantly, it can be fit into the solar cell's band structure. Commercialized and emerging thin-film photovoltaic (TFPV) technologies use metal oxides as transparent electrodes and as buffer or window layers [14-15]. The highly resistive intrinsic n-type zinc oxide (i-ZnO) buffer layer have been applied in many solar cell structures such as copper indium gallium selenide solar cell (CIGS), copper zinc tin sulfide (CZTS), and cadmium telluride (CdTe) solar cells and it significantly improves the device efficiency because it prevents leakage current and also functions as an anti-reflection coating which absorbs the ultraviolet part of the solar spectrum and permits the lower energy photons to move to the absorber layer [16-17]. Here, we demonstrated the structural, morphology and energy band gap investigation of i-ZnO nanofilm by varying the deposition condition.

2. MATERIAL AND METHODS

Zinc Oxide (ZnO) thin films layer were prepared by radio-frequency (RF) reactive magnetron sputtering method with ZnO purity of 99.99% as the target as shown in Figure 1. The sputtering chamber was evacuated at 1×10^{-5} Torr; then, prior to sputtering the target was employed to pre-sputtering around 5 minutes, in order to remove dust. The working pressure was kept stable at 1×10^{-2} Torr during the film deposition, with argon flow at 10 sccm and the sputtering power was maintained at 40 W. The substrate temperature was set to room temperature (25°C), this parameter is important to add atom mobility, desorption processes, and thermodynamic driving forces which affects phase stability and nucleation and growth phenomena. Thus, the deposition rate and microstructure of the developing film can be influenced by substrate temperature [18]. Sputtered ZnO films are typically crystalline already at room temperature (i.e. without intentional heating of the substrate). In this work, ZnO has been fabricated by altering the sputtering time in order to get layers with different thicknesses, where the thickness was varied between 50-200 nm. Note, the buffer layer thickness is one of the key factors to fabricate ZnO thin film with high crystalline quality and smooth surface. In sputtering system, the thickness of film can be controlled and varied depending on the sputtering gas pressure, the sputtering time, and the applied voltage [19]. The optical band gap (E_g) was determined by measuring the optical transmittance and absorbance coefficient from a UV/visible spectrophotometer. Furthermore, the crystal structure, texture and the grain size of the films were analysed using x-ray diffraction (XRD) measurement. Meanwhile the morphology of films was examined by field-emission scanning electron microscopy (FESEM) and Atomic force Microscopy (AFM).

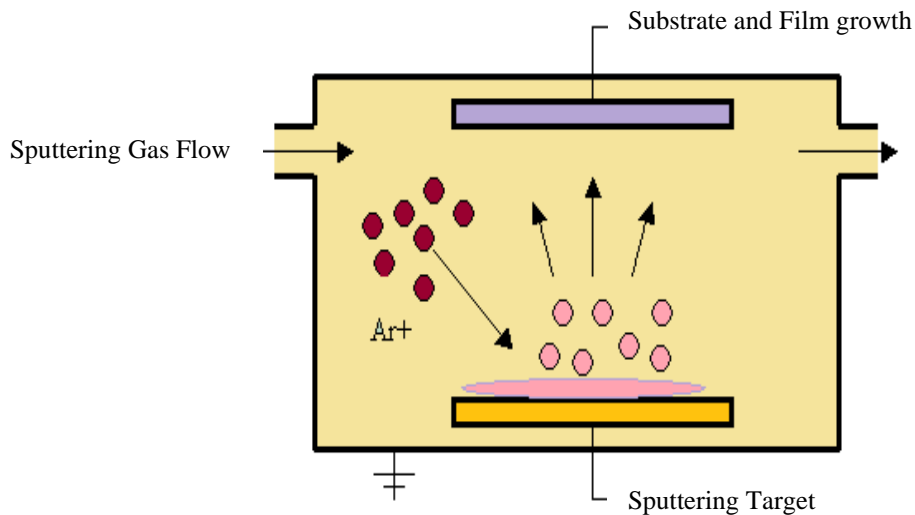


Figure 1. Schematic of ZnO nanofilm Sputtering Deposition System.

3. RESULTS AND DISCUSSION

3.1. The Structural Properties Results

The structural properties of ZnO thin film with different thickness were analyzed using X-Ray Diffraction (XRD). Figure 2 shows typical XRD patterns of ZnO films as-deposited at thickness of 50 nm, 80 nm, 100 nm, and 200 nm, respectively. The results show that the crystallinity of the films at thickness of 50 and 100 nm as confirmed by the XRD analysis and the stronger peaks were shown clearly when the thickness were at 50 nm and 200 nm. All of ZnO films as-deposited exhibit a (002) diffraction peak at 34.44, indicating that films have a hexagonal wurtzite structure and are preferentially oriented along the c-axis perpendicular to the plane of the substrate. Based on the XRD measurement results, ZnO thin films as-deposited grown by sputtering had a weak c-axis orientation except for films thickness at 50 nm and 200 nm. However, the (002) peak intensity of the sample with the buffer layer thickness of 50 nm is the strongest compared to others. The crystalline quality of ZnO thin films is significantly influenced by the buffer layer [20]. Assuming a homogeneous strain across the films, the crystallite size may be estimated from the full-width at half-maximum (FWHM) of (002) diffraction peak using Scherer's Formula:

$$D = 0.9\lambda / B \cos\theta \quad (1)$$

where D is the average crystalline size, λ is the wavelength of x-rays, and θ is Bragg's or diffraction angle of the x-rays, and B is the difference in angles at the FWHM value.

3.1.1. The Grain Size Result

The average grain size of as-deposited films of ZnO buffer layer in this study is in the range of 5.9–17 nm as shown in Table 1. The smallest FWHM was obtained for the sample with the thickness of 50 and 200 nm, indicating to have the best crystalline quality.

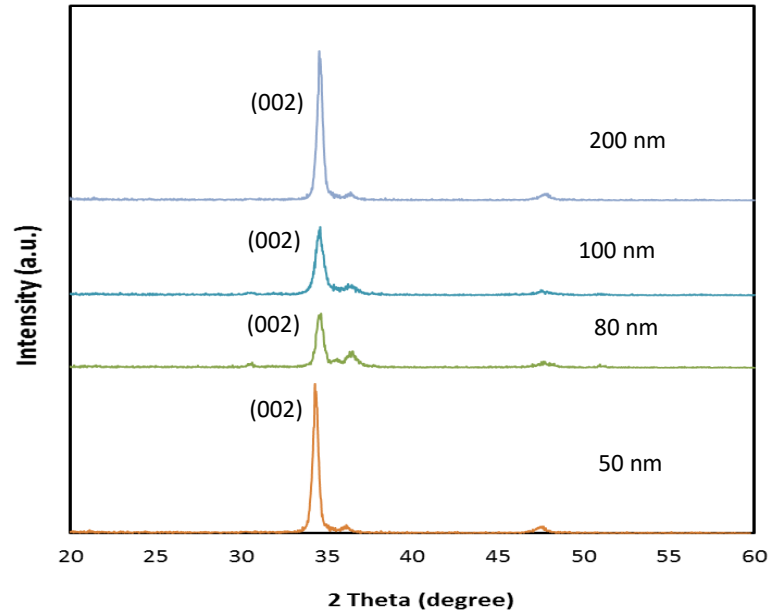


Figure 2. The typical XRD patterns of ZnO nanofilms as deposited

In previous work, Lee *et al.* reported that a smaller FWHM value means the larger the grain size. The crystal quality and the crystalline quality of ZnO nanofilm is significantly influenced by the buffer layer thickness [21]. Wang *et al.* has pointed that it was confirmed that film thickness as well as film crystallinity play decisive roles in optical transmittance [22-23]. These characteristics have an effect on the films, in particular to obtain better quality films of buffer layer for solar cell application.

Table 1 The Crystalline Size of ZnO nanofilm, dependent on the FWHM Value

| Sample ID | Thickness (nm) | FWHM (Rad) | Crystalline Size (nm) |
|-----------|----------------|------------|-----------------------|
| (a) | 50 | 0.00832 | 11.6 |
| (b) | 80 | 0.01622 | 8.5 |
| (c) | 100 | 0.02442 | 5.9 |
| (d) | 200 | 0.00124 | 17.3 |

The increase of grain size indicates the improvement of crystallinity of the film. Baek *et al.* pointed that as a result, thickness of ZnO nanofilm plays an important role in changing the crystallinity. Therefore, it is necessary to consider the correlation between thickness of film and crystallinity in fabricating various ZnO based devices. Therefore, to assure the high performance of ZnO-based devices, it is very important to fabricate ZnO films with high crystalline quality and smooth surfaces.

3.2. Morphology/Surface Roughness

3.2.1 AFM Surface Roughness

In order to investigate the morphological properties of ZnO thin films at different thickness, the morphology of ZnO films was imaged using Atomic Force Microscopy (AFM) as shown in Figure 3. AFM examination was carried out to evaluate the effect of thickness variation and annealing temperature on the surface topology of ZnO nanofilms. The average roughness of as-deposited

ZnO thin films is shown in Figure 3; the root-mean-square (RMS) values of surface roughness was found to be 4.74, 4.55, 2.97 and 9.34 nm, respectively. The surface roughness for all as-deposited ZnO nanofilms in this range values indicated that the film have smooth surface. The smooth surface roughness is one of the qualities that contribute in making ZnO thin film an ideal buffer layer in solar cells.

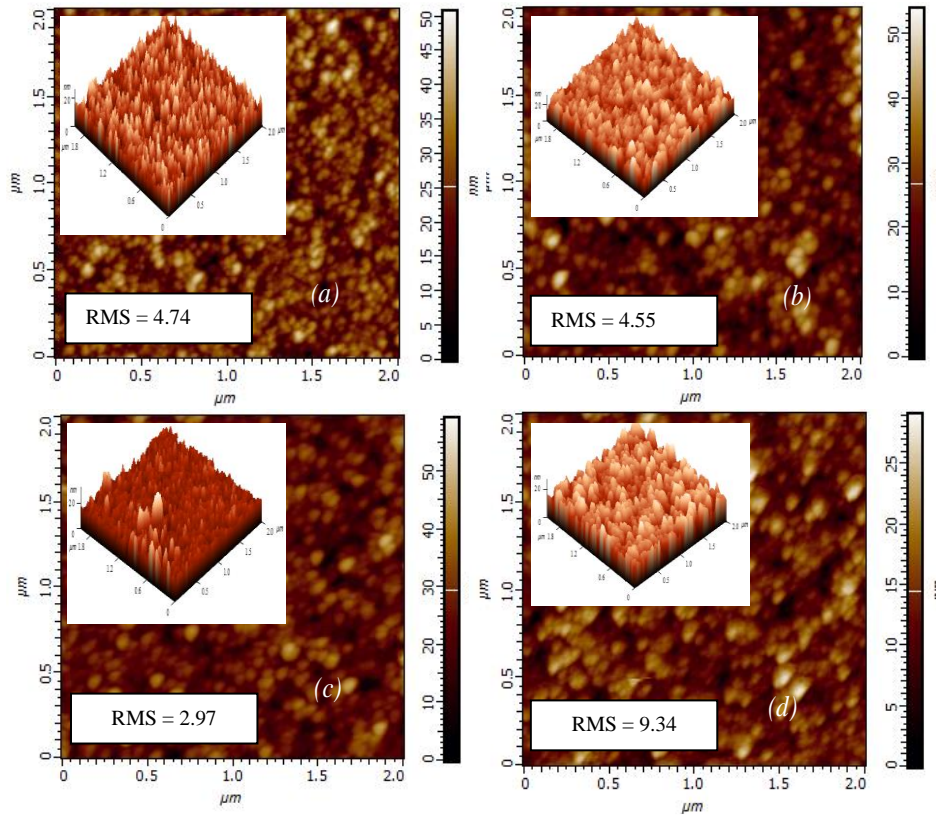


Figure 3. AFM images of ZnO deposited films with different thicknesses; (a) 50 nm, (b) 80 nm, (c) 100 nm and, (d) 200 nm.

The biggest root mean square (RMS) value of surface roughness of as-deposited film is 9.34 nm at 200 nm thick and the lowest roughness value was 2.97 nm with 100 nm thick sample. This indicates that with increase of nanofilm, the surface roughness of the film also increases.

3.2.2 FESEM Characterization Result

In order to investigate the morphological properties of ZnO thin films at different thicknesses, the morphology of ZnO films was imaged by FESEM as shown in Figure 4. The surface of as-deposited sample was shown to be homogenous with no holes due to the good recrystallized films which caused the epitaxy quality to improve. It shows that as thickness of film increases up to 200 nm, the grain size of ZnO thin films also increases, as an evidence that the surface morphology varies when the thickness of films is changed. Hence, in terms of the crystallinity of ZnO thin films, the FESEM analysis is consistent with that of the XRD analysis. The increase of the grain size indicates the improvement of crystallinity of the film [24].

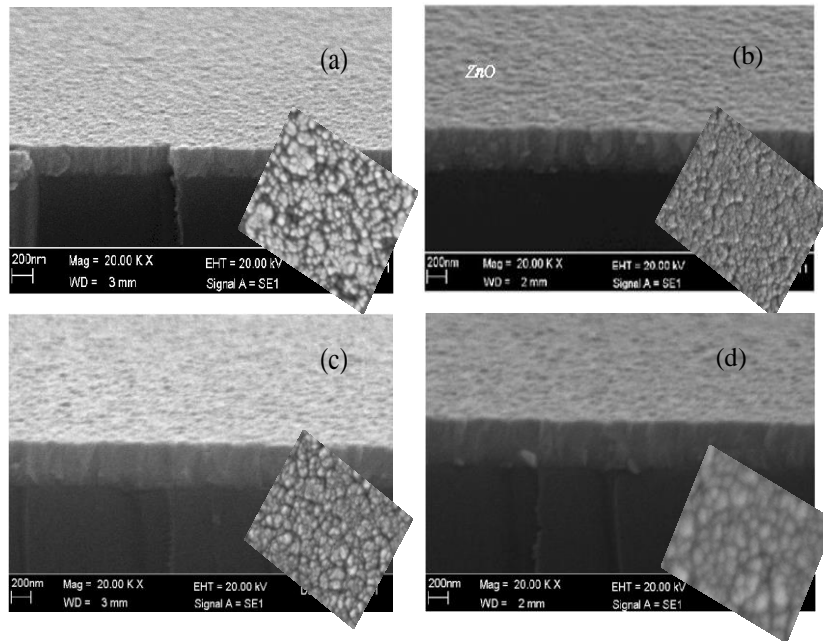


Figure 4. FESEM images of i-ZnO nanofilms with different thicknesses; (a) 50 nm, (b) 80 nm, (c) 100 nm and, (d) 200 nm.

In addition, Baek *et al.* have pointed out that the thickness of ZnO nanofilm plays an important role in changing the crystallinity [13]. It is necessary to consider the correlation between thickness and the crystallinity of film in fabricating ZnO buffer layer-based devices, due to both of those parameters play an important role in changing the crystallinity [24].

3.3. The Optical Properties and the Band Gap Energy Of Intrinsic ZnO Nanofilms

The optical absorption and transmission spectra measurements of ZnO nanofilm samples were performed using an Ultraviolet-Visible-Infrared (UV-Vis) in the range of wavelength of 350 to 900 nm, and the results are shown in Figure 5 and Figure 6. The optical absorption edge was found to shift to the shorter wavelength with the increase in the film thickness and all the ZnO thin films show about 80% optical transmission in the visible region.

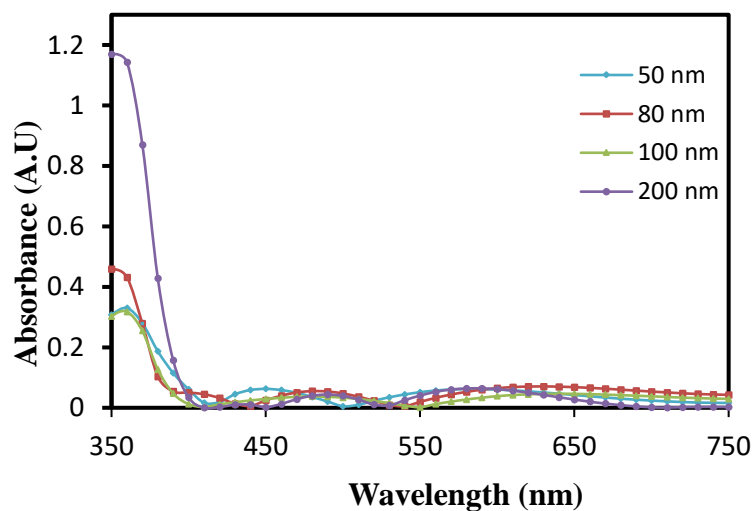


Figure 5. The Optical spectra absorbance of i-ZnO at different thicknesses; (a) 50 nm, (b) 80 nm, (c) 100 nm and, (d) 200 nm.

Meanwhile for the transmittance results, it was demonstrated that the films showed over 90% transmittance in the UV region and around 75-83% transmittance in the visible region. However, the transmittance of films decreases considerably with increasing film thickness except for i-ZnO sample which was 200 nm thick. As reported previously, the film thicknesses as well as film crystallinity play decisive roles in optical transmittance as well [21]. Therefore, to assure the high performance of i-ZnO-based devices, it is very important to fabricate ZnO films with high crystalline quality and smooth surface. These characteristics have an effect on the films in particular to obtain better quality films for buffer layer in TFSC application.

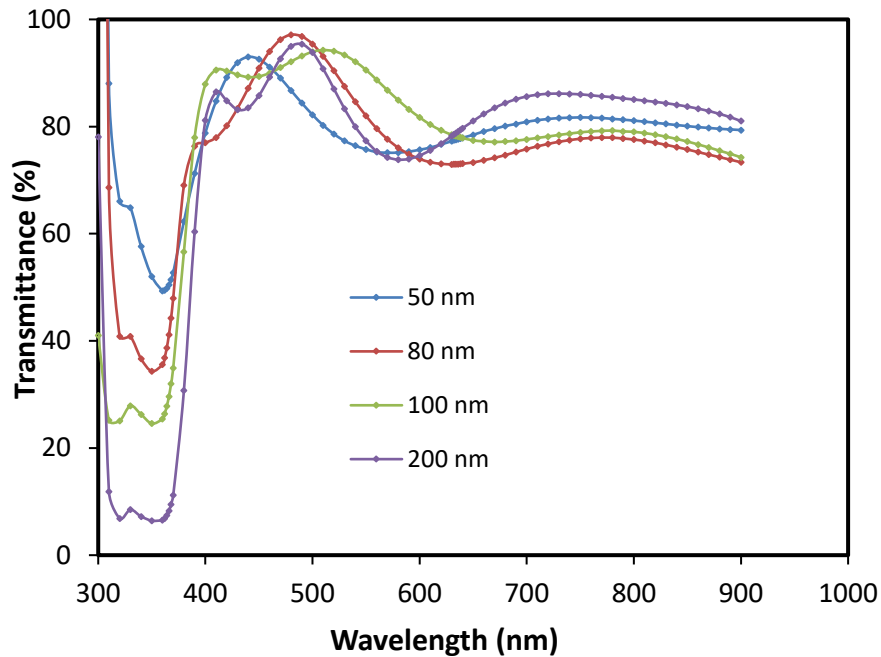


Figure. 6. The Optical spectra transmittance of i-ZnO with different thicknesses ; (a) 50 nm, (b) 80 nm, (c) 100 nm and, (d) 200 nm.

Furthermore, the variation of absorption coefficient, α with respect to photon energy ($h\nu$) was found to obey the relation: $\alpha h\nu = A(h\nu - E_g)^{1/2}$ for the allowed direct transition where A is the edge width parameter and E_g is the optical band gap. The optical band gap of ZnO thin films has been determined using the formula for the direct band gap semiconductors and the equation is expressed as follows:

$$\alpha h\nu = A(h\nu - E_g)^{1/2} \quad (2)$$

where α is the absorption coefficient, $h\nu$ is the photon energy, A is the constant and E_g is the optical band gap. The optical band gap values are obtained by extrapolating the linear portion of the plots of $(\alpha h\nu)^2$ versus $h\nu$ to $\alpha = 0$, as shown in Figure 7. Based on the investigation of properties of ZnO thin films deposited under different thicknesses, the band gap of ZnO thin films can be adjusted from 3.14 eV to 3.25 eV. In this work, the optical properties were used for characterizing the undoped ZnO thin films; and we found that the stoichiometric ZnO nanofilms were highly transparent and have a good optical band gap.

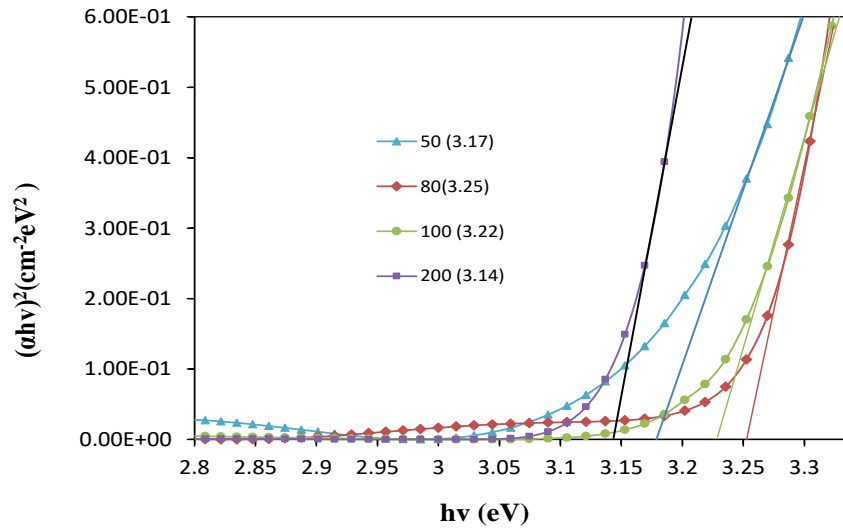


Figure 7. Derivation of energy band gap of i-ZnO for different thicknesses; (a) 50 nm, (b) 80 nm, (c) 100 nm and, (d) 200 nm.

There are several important criteria that need to be considered when selecting a suitable buffer material, and one of them is having a wide band gap (E_g), and suitable conduction band alignment. Therefore the E_g of the buffer layer should be wide enough to avoid undesirable absorption of the solar spectrum, for example, the normally used indium tin oxide (ITO) window layer in the CIGS devices have E_g values over 3.3 eV which means the buffer material should be close or have a similar bandgap value to allow the short wavelength light to reach the absorber layer material. As reported in previous work, the researchers studied the new correlation of the crystallite size in undoped ZnO thin film with the band gap energy. They found that the crystallite sizes calculated from the ZnO thin films are mainly influenced by the band gap energy of the thin films. Furthermore, the crystallite size can be estimated by the optical gap energy with substrate temperature [25]. Figure 8 shows the relation between the i-ZnO nanofilm thicknesses and the obtained energy band gap, the transmittance, the surface roughness and the grain size.

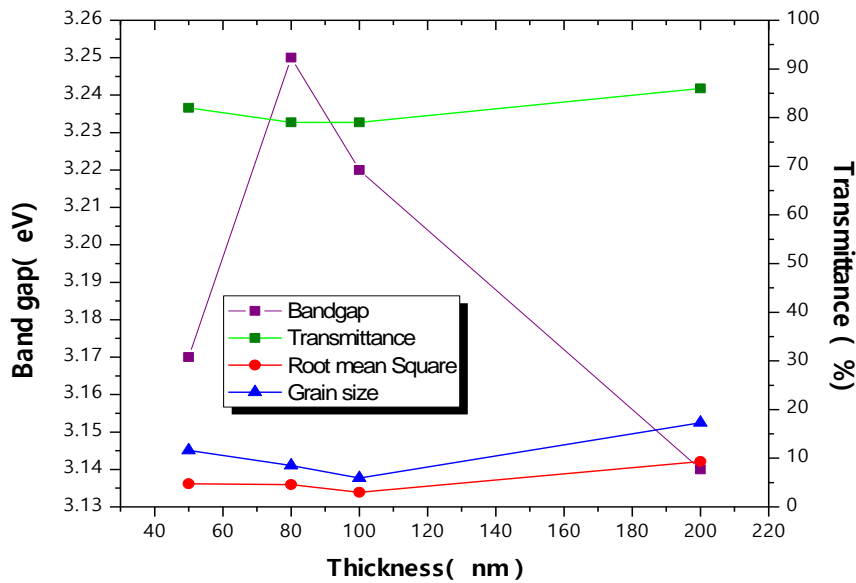


Figure 8. Derivation of energy band gap, RMS, transmittance and grain size of i-ZnO for various nanofilm thicknesses.

Based on our investigation, it's clearly shown that the achieved band gap results were connected to the grain size result, or vice versa. As observed, the wide band gap was achieved when the layer thickness of i-ZnO buffer layer was set at low thicknesses of below 100 nm. Our future work will involve using the i-ZnO layer in TFSC device characterization.

4. CONCLUSION

The effects of deposition parameters causing various thicknesses of i-ZnO nanofilms on its optical and structural properties were discussed. The crystallinity, optical and the band gap of thin films can be simply adjusted by controlling the thickness during RF-sputtering processes. The ZnO films had a hexagonal wurtzite structure and the crystallinity improved whereas the c-axis crystalline size increases with the increase of film thickness. Based on the investigation of properties of ZnO thin films deposited under different thickness, the band gap of ZnO thin films can be adjusted from 3.14 eV to 3.25 eV with increasing thickness from 50 nm to 80 nm. The surface roughness for all as-deposited ZnO thin films were in the range of 2.97 nm – 9.34 nm, indicated that the film have smooth surface. It was found that the properties of the deposited ZnO were highly dependent on the parameters deposition conditions, such as, adjusted the film thickness, Sputtering Power, substrate condition, vacuum process and etc. The combination of lower films thickness, high transmittance, good crystallinity and low surface roughness are the key factor or the goals target in fabrication/deposition of films layer, then as those factor achieved then automatically that makes the ZnO thin films a promising low cost buffer layer for thin film solar cell devices (CIGS, CdTe and CZTS solar cells).

ACKNOWLEDGEMENTS

We acknowledge the technical support given by Institute of Microengineering and Nanoelectronics (IMEN), UKM. This research was funded in-part by the Ministry of Higher Education Malaysia using grant FRGS/1/2019/STG02/UKM/02/8, LRGS/2015/UKM-UKM/NANOMITE/04/01 as well as Universiti Kebangsaan Malaysia Grant number DIP-2016-022. This publication is also supported by the ASEAN-India Development Fund (AISTDF) by DST-SERB, Govt. of India (RR-2020-002).

REFERENCES

- [1] B. A. Badr, Q. Q. Mohammed, N. H. Numan, M. A. Fakhri, A. W. Wahhab, International Journal of Nanoelectronics and Materials. **12** (2019) 283-290.
- [2] A. M. Holi, A. A. Al-Zahrani, International Journal of Nanoelectronics and Materials. **13** (2020) 121-130.
- [3] A. Sharmin, S. Tabassum, M. S. Bashar, Z. H. Mahmood. Journal of Theoretical and Applied Physics. **13** (2019) 123-132
- [4] S. M. Gan, P. S. Menon, G. Hegde. Materials Research Express. **7** (2020) 1-16
- [5] A. R. A Rashid, P. S. Menon, S. Shaari, Optoelectronics and Advanced Materials, Rapid Communications **7** (2013) 835-839
- [6] G. S. Mei, N. R. B Mohamad, N. A. B Jamil, B. Y. Majlis, P. S. Menon, Sains Malaysiana **47** (2018). 2565–2571
- [7] H. Ghaffari, A. Tavakoli, A. Moradi, A. Tabarraei, *et al.* Journal of Biomedical Science. **26** (2019) 1-10
- [8] J. S. Wellings, N. B. Chaure, S. N. Heavens, I. M. Dharmadasa, Journal of Thin Solid Films. **516** (2008) 3893-3898.
- [9] P. Malkeshkumar, K. Hong-Sik, J. Kima, Y. Ju-Hyung, S. J. Kim, E. H. Choi, H-H. Park. Solar Energy Materials and Solar Cells **170** (2017) 246–253.

- [10] X. Liu, L. Gu, Q. Zhang, J. Wu, Y. Long, Z., *Nat. Commun.* **5** (2014) 1-9.
- [11] H. Chen, K. Liu, L. Hu, A. A. Al-Ghamdi, X. Fang. *Today.* **18** (2015) 493–502.
- [12] Z. Wang, R. Yu, C. Pan, Z. Li, J. Yang, F. Yi, *et al.* *Nat. Commun.* **6** (2015) 1-7.
- [13] C. S. Baek, D. H. Kim, H. H. Kim, K. J. Lim. *Journal of Ceramic Processing Research.* **13** (2012) 403-406.
- [14] L. W. Rieth. Ph.D. Thesis, Graduate School of the University Of Florida (2001), USA.
- [15] S. M. Sze, K. K. Ng, *Physics of Semiconductor Devices*, Canada (2006), Wiley.
- [16] J. Husna, M. M. Aliyu, A. M. Islam, P. Chelvanathan, N. H. Radhwa, S. H. Karim, M. M. R. Amin, *N. Energy Procedia.* **25** (2012) 55-61.
- [17] S. Alhammadi, H. Park, W. K. Kim, *Materials.* **12**, 1365 (2019).
- [18] X. Wang, X. Zeng, D. Huang, X. Zhang, Q. Li, *Journal of Mater. Sci. Mater. in Electronics.* **23** (2012) 1580-1586.
- [19] Y. Hamakawa. *Thin-Film Solar Cells: Next Generation Photovoltaics and its Applications*, Berlin, Germany; Springer (2004).
- [20] S. Valliyil, A. Iqbal, C. Kien, A. Iacopi, F. Mohd-Yasin, *Micromachines.* **8** (2017).
- [21] G. H. Lee, *Journal of Ceramic Processing Research.* **13** (2012)
- [22] X. Wang, X. Zeng, D. Huang, X. Zhang, Q. Li, *Journal of Mater. Sci. Mater. in Electronics.* **23** (2012) 1580-1586.
- [23] D. Wang, Ph.D. Thesis, Department of Electronic and Photonic System Engineering, Kochi University of Technology, Japan (2012).
- [24] B. Z. Dong, G. J. Fang, J. F. Wang, W. J. Guan, X. Z. Zhao, *Journal of Appl. Phys.* **101** (2007) 3713 - 3717.
- [25] A. Abedini, M. Saraji, A. A. A. Bakar, P. S. Menon, S. Shaari, *Plasmonics.* **13** (2018) 771-778.